AKR1B10 inhibits the proliferation and metastasis of hepatocellular carcinoma cells by regulating the PI3K/AKT pathway

KE TIAN[1], YING DENG[1], ZHIPENG LI[2], HUAXIN ZHOU[2] and HUI YAO[1]

[1]Second Department of General Surgery, No. 2 People's Hospital of Lanzhou, Lanzhou, Gansu 730030;
[2]Department of Hepatobiliary Surgery, The Second Hospital of Shandong University, Jinan, Shandong 250000, P.R. China

Abstract. Hepatocellular carcinoma (HCC) is one of the most frequent and aggressive malignant neoplasms, and is associated with a poor prognosis. Therefore, there is a crucial need to develop novel cancer therapies and identify novel therapeutic targets. Aldo-keto reductase family 1 member B10 (AKR1B10) is expressed in various types of cancer. However, the role of AKR1B10 in the pathological process of HCC and its underlying molecular mechanism is poorly understood. AKR1B10 expression was evaluated pan-cancer and in HCC using the Genomic Data Commons-The Cancer Genome Atlas (GDC-TCGA) and International Cancer Genome Consortium (ICGC) databases. The relationship between elevated AKR1B10 expression and overall survival in HCC patients was analyzed using a Kaplan-Meier plot. The effects of AKR1B10 on the proliferation, migration, and invasion of HCC cells were evaluated. The proliferation of HCC was measured using CCK-8 and colony formation assays. Transwell and wound healing assays were used to assess the migration and invasion of HCC cells. Western blots were used to detect the expression of proliferative and epithelial-mesenchymal transition (EMT) related proteins in HCC cells, including CCND1, E-cadherin, N-cadherin, vimentin, Twist1, PI3K/p-PI3K, and AKT/p-AKT. AKR1B10 expression was significantly upregulated pan-cancer and in liver cancer. Upregulated AKR1B10 expression was associated with a worse overall survival. HCC cell proliferation, migration, and invasion were found to be influenced by AKR1B10 activity, as demonstrated using DepMap analysis. AKR1B10 knockdown in Huh7 cells reduced proliferation, migration, invasion, and EMT. Mechanistically, AKR1B10 increased the expression of proliferative and EMT-related proteins CCND1, E-cadherin, N-cadherin, vimentin, and Twist1. PI3K and AKT phosphorylation levels decreased following AKR1B10 knockdown. In conclusion, AKR1B10 promoted the proliferation, migration, and invasion of HCC cells via the PI3K/AKT signaling pathway, a potential prognostic indicator.

Introduction

Hepatocellular carcinoma (HCC), the most common form of liver cancer, is one of the most frequently diagnosed malignant neoplasms worldwide (1,2). In recent decades, HCC has received a significant amount of attention due to the rapid rise in HCC-associated mortality (1,3). Despite advances in diagnostic techniques and therapeutic strategies over the last decade, the prognosis of patients with HCC has remained poor (4,5). The majority of HCC patients are diagnosed in the first instance with advanced-stage HCC; therefore, the estimated 5-year overall survival rate is <20% (6). Previous studies have shown that the prognosis of HCC is associated with several factors, including the heterogeneity of HCC (7), diagnostic challenges (8), limited radiation therapy, and the development of resistance to HCC. Thus, additional research into the molecular mechanisms driving the malignant transformation of hepatocytes is urgently needed.

Aldehyde ketone reductase (AKR) family member B10 (AKR1B10) belongs to the AKR1B subgroup (9). AKR1B10 is a cytosolic NADPH-dependent reductase, catabolizing various endogenous compounds by catalyzing the corresponding redox reactions (2). According to recent studies, expression of this enzyme is upregulated in several types of cancer, including adrenocortical (10), breast (11), colon (12), and hepatocellular carcinoma (13,14). AKR1B10 has significant potential as a relevant biomarker and therapeutic target for predicting tumor progression. Based on a large-scale proteome quantification analysis, HCC tissues showed dysregulated AKR1B10 expression compared with normal liver (15,16). However, the specific function of AKR1B10 in HCC pathology and its molecular mechanisms remain to be determined.

The present study examined the diagnostic performance of AKR1B10 in HCC tumor tissues. Furthermore, the role and mechanism of AKR1B10 in the proliferation, migration,

invasion, and epithelial-mesenchymal transition (EMT) of HCC cells was examined.

Materials and methods

Public data acquisition. The genomics data of GSE146719/GPL20795 was downloaded from the Gene Expression Omnibus (GEO) database and analyzed using the DESeq2 package (version 1.39.8; https://www.ncbi.nlm.nih. gov/geo/). Normalized RNA-seq data (HTSeq-FPKM) and survival data of the Pan-Cancer Atlas (PANCAN) and the liver hepatocellular carcinoma (LIHC) project of The Cancer Genome Atlas (TCGA) were accessed from the GDC website (https://portal.gdc.cancer.gov/) on March 1, 2023, and the data set is referred to as GDC-TCGA-LIHC in this article. Normalized gene expression (normalized_read_count) and donor information of the liver cancer project (named: LIRI-JP) of the International Cancer Genome Consortium (ICGC) were downloaded from the ICGC data portal (https://dcc.icgc.org/), and the data set is referred to in this article as ICGC-LIRI. Immunohistochemical images of AKR1B10 in tumor samples were analyzed and accessed from The Human Protein Atlas database website (https://www.proteinatlas.org/). The gene effect and expression of HCC cell lines were analyzed and downloaded from the Broad Institute DepMap website (https://depmap.org/).

Public data processing. Normalized quantification of gene expression in GDC-TCGA-LIHC was converted into transcripts per million (TPM) and then logarithmically transformed $[\log_2(TPM+1)]$. In ICGC-LIRI, the expression values were directly $\log_2$ (normalized_read_count) transformed since they were all >0 (17). No normal samples were included in the prognosis analysis in GDC-TCGA-LIHC and ICGC-LIRI. Missing values were considered in the GDC-TCGA dataset if the clinical information of patients was unavailable or unknown.

Cells and agents. Human HCC cell lines Huh7 and Hep3B were obtained from the Cell Bank of the Chinese Academy of Sciences and cultured in DMEM (Thermo Fisher Scientific, Inc.), supplemented with 10% FBS (Thermo Fisher Scientific, Inc.), and 1% penicillin/streptomycin (HyClone, Cytiva; cat. no. SV30010) at 37°C with 5% CO_2. HCC cells were authenticated via short tandem repeat analysis. Mycoplasma-free cells were used in all experiments.

Cells were seeded into six-well plates ($3-5x10^5$ cells/well). Sh/oe-AKR1B10 in HCC cells was performed using the lentivirus (DNA:16 μg/100 ml; Shanghai GenePharma Co., Ltd.), when the cell confluency reached 60-70%. The cells were treated with 100 μl/ml ($1x10^9$ TU/ml) lentivirus for 8 h. Stably transduced cell lines were selected with 4 μg/ml puromycin (YEASEN, China). Full-length AKR1B10 sequences were ligated into the lentivirus vectors pCMV-3xHA. The shRNA sequences (5'-3') were as follows: shAKR1B10, CGCTCC TACTGACTCCTATTT, and Scramble, CCTAAGGTTAAG TCGCCCTCG. The reagents and antibodies used are given in Table I.

Cell proliferation and colony formation assays. HCC cell proliferation was assessed using CCK-8 assays (Beyotime

Institute of Biotechnology). Briefly, $3-5x10^3$ stable cells transfected with sh/oeAKR1B10 or corresponding scramble oligos were plated into 96-well plates and incubated for 4 days.

The cells were seeded in 12-well plates ($1x10^4$ cells/well) for 2 weeks to determine colony formation. The methanol-fixed colonies were then stained with crystal violet solution at room temperature.

Wound healing assay. Transfected Huh7 cells were seeded into six-well plates ($1x10^5$ cells/well). With a 10 μl pipette tip, wounds were made when the cell confluency reached 80-90%, and the cells were cultured in serum-free DMEM at 37°C. The wounds were observed under an inverted light microscope (x100). ImageJ v1.8.0 (National Institutes of Health) was used to evaluate the cell migration rate as follows: Wound closure surface area/wound total surface area x100%.

Western blot and analysis. Using RIPA buffer and PMSF (Beyotime Institute of Biotechnology) with phosphatase inhibitor (Beijing Solarbio Science & Technology Co., Ltd.), total cell proteins were extracted and analyzed by western blotting. Briefly, proteins (40 μg) were loaded onto 10% SDS-PAGE for electrophoresis and transferred to polyvinylidene difluoride membranes (MilliporeSigma). Membranes were blocked with 5% BSA at room temperature for 1 h and then incubated with primary antibodies overnight at 4°C and then secondary antibodies at 37°C for 1 h, according to the manufacturer's recommendations. Finally, the protein levels were confirmed using enhanced chemiluminescence (Tanon 4800; Tanon Science and Technology Co., Ltd.) and normalized with an anti-GAPDH antibody. The images were analyzed using ImageJ (version 1.8.0.345, National Institutes of Health).

Transwell migration and invasion assays. Typically, $1x10^5$ transfected Huh7/Hep3B cells in serum-free media were seeded into the upper chambers with (invasion) or without (migration) Matrigel coating (diluted in DMEM; Corning, Inc.), and the bottom chambers were filled with 600 μl supplemented DMEM medium. After 36 h, the cells that had migrated and invaded through to the bottom of the inserts were fixed with methanol and stained with crystal violet for 30 min at room temperature, respectively. In five random fields of view, the numbers of cells that had migrated/invaded were viewed under an inverted light microscope (magnification, x200) and imaged and quantified.

Flow cytometry analysis. For cell cycle analysis, cells were fixed with 70% ethanol (4°C, >30 min), washed with PBS (5 min, 3 times), and then stained with RNase/PI staining solution (room temperature, 30 min). Flow cytometry (Beckman Coulter, Inc.) was used to measure the DNA content (>10,000 cells per sample), and ModFIT LT v3.1 software (Verity Software House, Inc.) was used for analysis.

Statistical analysis. GraphPad Prism version 8.0 (GraphPad Software, Inc.) was used for statistical analysis. ImageJ was used for densitometry analysis. Comparisons between groups were assessed using a Student's t-test or an ANOVA followed by a post-hoc Tukey's test for multi-group comparison. $P<0.05$ was considered to indicate a statistically significant difference.

Table I. Reagents and antibodies used in the present study.

| Reagent or antibody	Source	Cat. no.
AKR1B10	Abcam	ab192865
EMT antibodies kit	Cell Signaling Technology, Inc.	9782T
PI3K	Cell Signaling Technology, Inc.	84249T
p-PI3K	Cell Signaling Technology, Inc.	4228S
AKT	ProteinTech Group, Inc.	60203-2-lg
p-AKT	ProteinTech Group, Inc.	66444-1-lg
p-eIF4EBP1	Abcam	ab259329
p-RPS6	Abcam	ab80158
GAPDH	Abcam	ab181602
GDC-0941	Calbiochem (Merck KGaA)	957054-30-7
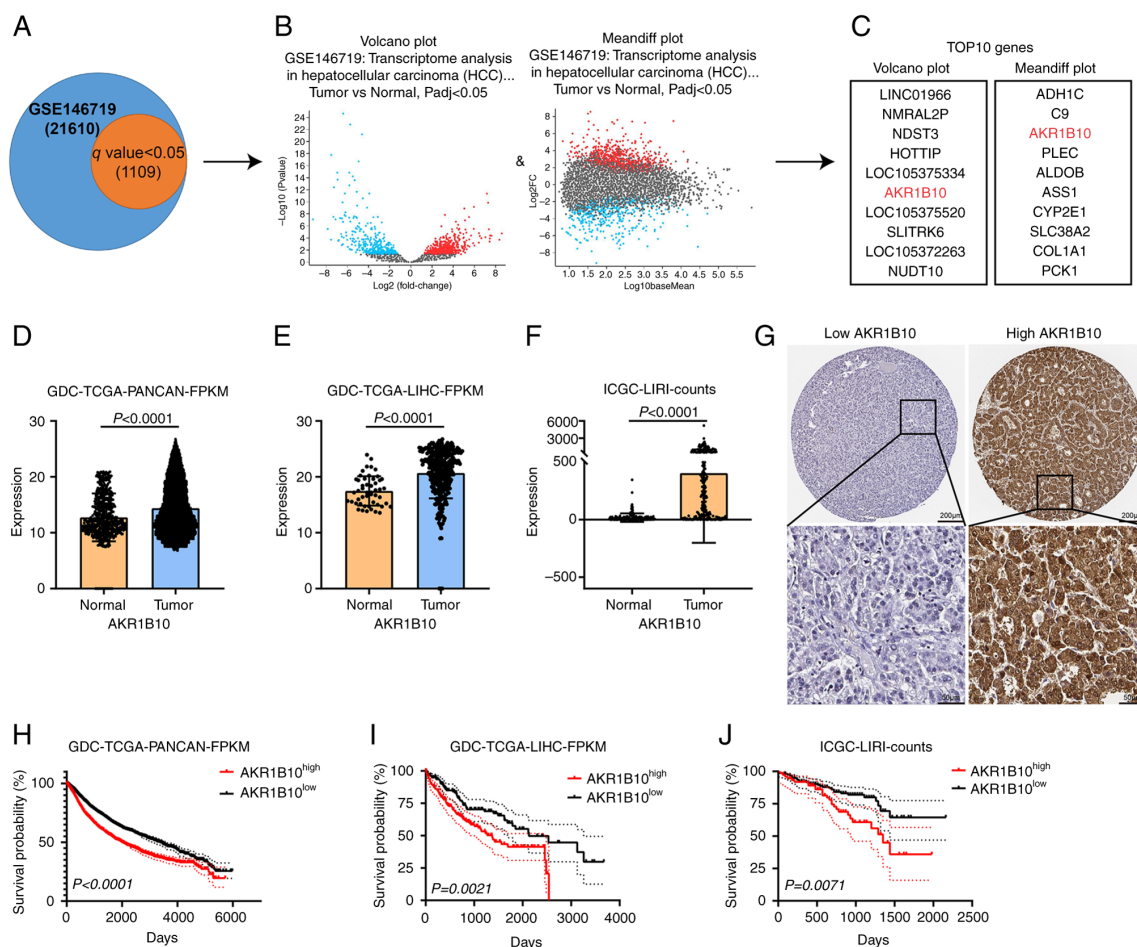
Figure 1. AKR1B10 expression was screened out and found to be upregulated in hepatocellular carcinoma. (A-C) Flow chart of AKR1B10 filtering from the GSE146719 dataset (D-F) Amplification of AKR1B10 was common in the GDC-TCGA and ICGC provisional cohort. (G) Representative images of immunohistochemical staining for low/high expression of AKR1B10 in public tissue microarray datasets from The Human Protein Atlas database (upper image: magnification, x100, scale bar, 200 μm; lower image: magnification, x400; scale bar, 50 μm). (H-J) Prognostic significance of AKR1B10 in (H) GDC-TCGA-PANCAN, (I) GDC-TCGA-LIHC, and (J) ICGC-LIRI cohorts. AKR1B10, aldo-keto reductase family 1 member B10; GDC-TCGA, Genomic Data Commons-The Cancer Genome Atlas; ICGC, International Cancer Genome Consortium; PANCAN, Pan-Cancer Atlas; LIHC, liver hepatocellular carcinoma; LIRI, donor information of the liver cancer project; FPKM, Fragments Per Kilobase Million.

Results

AKR1B10 was screened out and was found to be upregulated in HCC. To evaluate the biological implications of the differential expression of genes in HCC vs. normal liver tissues, expression analysis in the GSE146719 dataset was performed. Moreover, 1,109 genes with q-value (p.adj) <0.05 were selected for subsequent processing (Fig. 1A). Deep analysis of these genes was
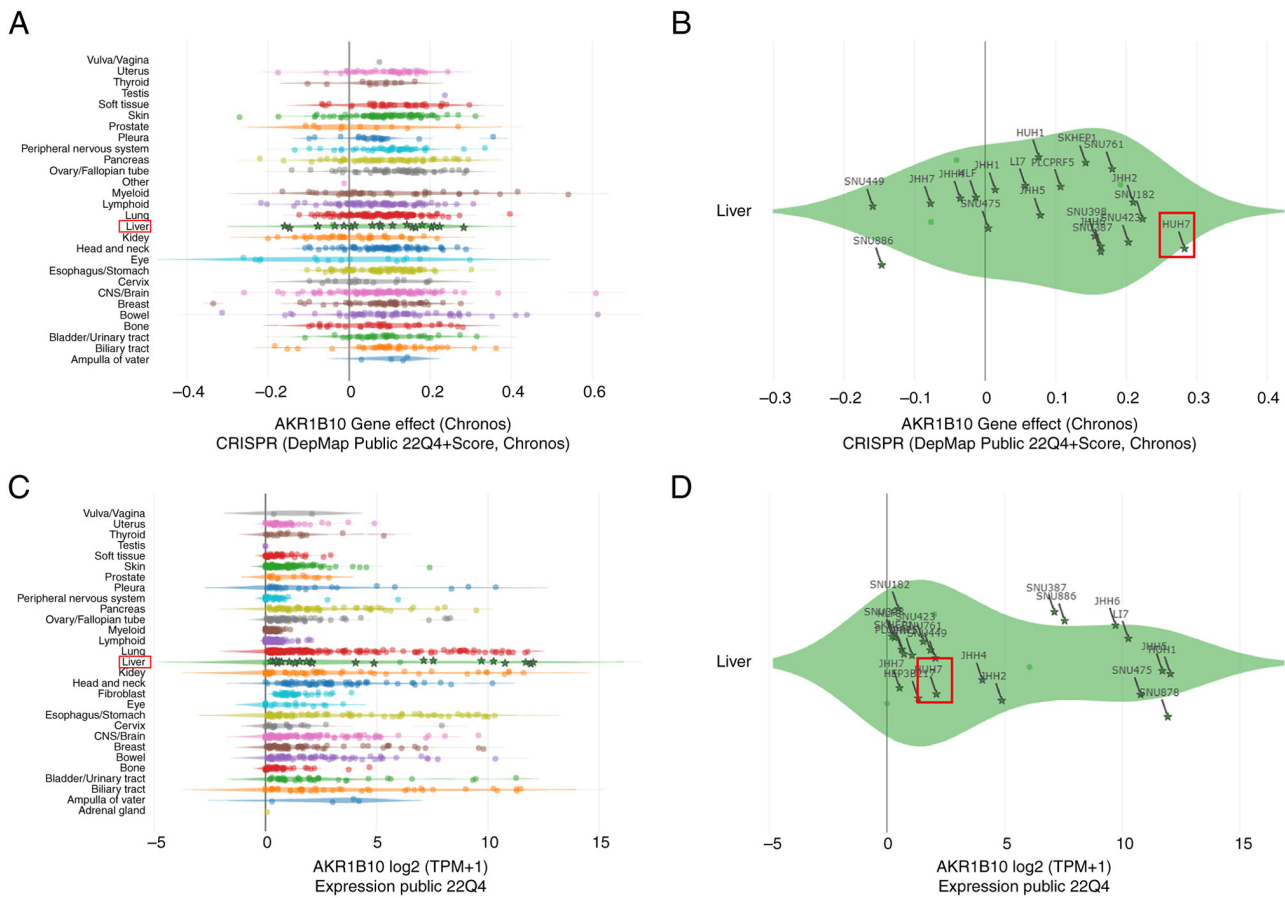
Figure 2. DepMap analysis of AKR1B10. (A and B) The Gene Effect CRISPR (DepMap Public 22Q4 + Score, Chronos) and (C and D) the expression of AKR1B10 in hepatocellular carcinoma cell lines with the DepMap dataset was validated. AKR1B10, aldo-keto reductase family 1 member B10.

performed using a volcano plot and mean differential plot maps (Fig. 1B). The top 10 genes from the above-analyzed data were selected for repeated analysis. Subsequently, the AKR1B10 was screened out. AKR1B10 status in HCC by exploring its expression in this disease. Higher AKR1B10 expression in pan-cancerous tissues suggested that this oncogene may be upregulated during the development of HCC. As shown in Fig. 1E and F, AKR1B10 expression in HCC tissues was significantly higher than in normal liver tissues. Combined with the public IHC datasets from The Human Protein Atlas database, the expression and localization of AKR1B10 were detected. AKR1B10 was primarily expressed in the cytoplasm (Fig. 1G), consistent with its function as an enzyme catalyzing redox reactions. HCC patients were divided into two groups based on the median value of AKR1B10 expression in GDC-TCGA-PANCAN and GDC-TCGA-LIHC datasets, and patients labeled as low-AKR1B10 had significantly longer survival than the remaining high-AKR1B10 (Fig. 1H and I; $P<0.0001$ and $P=0.0021$, respectively). Similarly, patients classified with the low-AKR1B10 group had a significantly better prognosis in the ICGC-LIRI dataset (Fig. 1J; $P=0.0071$). Thus, high expression of AKR1B10 in HCC patients was associated with poorer outcomes, and AKR1B10 was shown to be a useful biomarker for the disease (13,16).

DepMap analysis of AKR1B10. Due to the differential expression of AKR1B10 and its prognostic value in HCC, its potential functions in this disease were examined. Using

the DepMap dataset, a gene effect CRISPR (DepMap Public 22Q4 + Score, Chronos) analysis of this gene was performed. The results showed a significant gene effect of AKR1B10 in most HCC cell lines (Fig. 2A), especially in Huh 7 cell line (Fig. 2B). Next, the expression of AKR1B10 in HCC cell lines was analyzed using the DepMap dataset. The results showed that AKR1B10 was expressed at differentially high levels in all HCC cell lines, including Huh7 (Fig. 2C and D). The above results indicated that AKR1B10 was highly expressed in HCC tissues and showed a significant gene effect in HCC and Huh7 cells, and thus these cells were selected as an ideal HCC cell line for further experimental validation.

AKR1B10 promotes the proliferation, migration, and invasion of HCC cells. After transfection of sh-AKR1B10 into Huh7 cells, AKR1B10 expression was significantly decreased (Fig. 3A). AKR1B10 knockdown significantly reduced Huh7 cell viability and proliferation in CCK-8 and colony formation assays (Fig. 3B and C). Further studies illustrated that AKR1B10 promoted the migration and invasion of Huh7 cells in wound healing and Transwell assays (Fig. 3D-F). In addition, the above effects of AKR1B10 overexpression on Hep3B, a relatively low-expressing AKR1B10 HCC cell line, were assessed. The results showed that cellular activity was significantly promoted in Hep3B cells (Fig. 3G-I). The above results suggested that AKR1B10 played a prominent role in the proliferation, migration, and invasion of HCC.
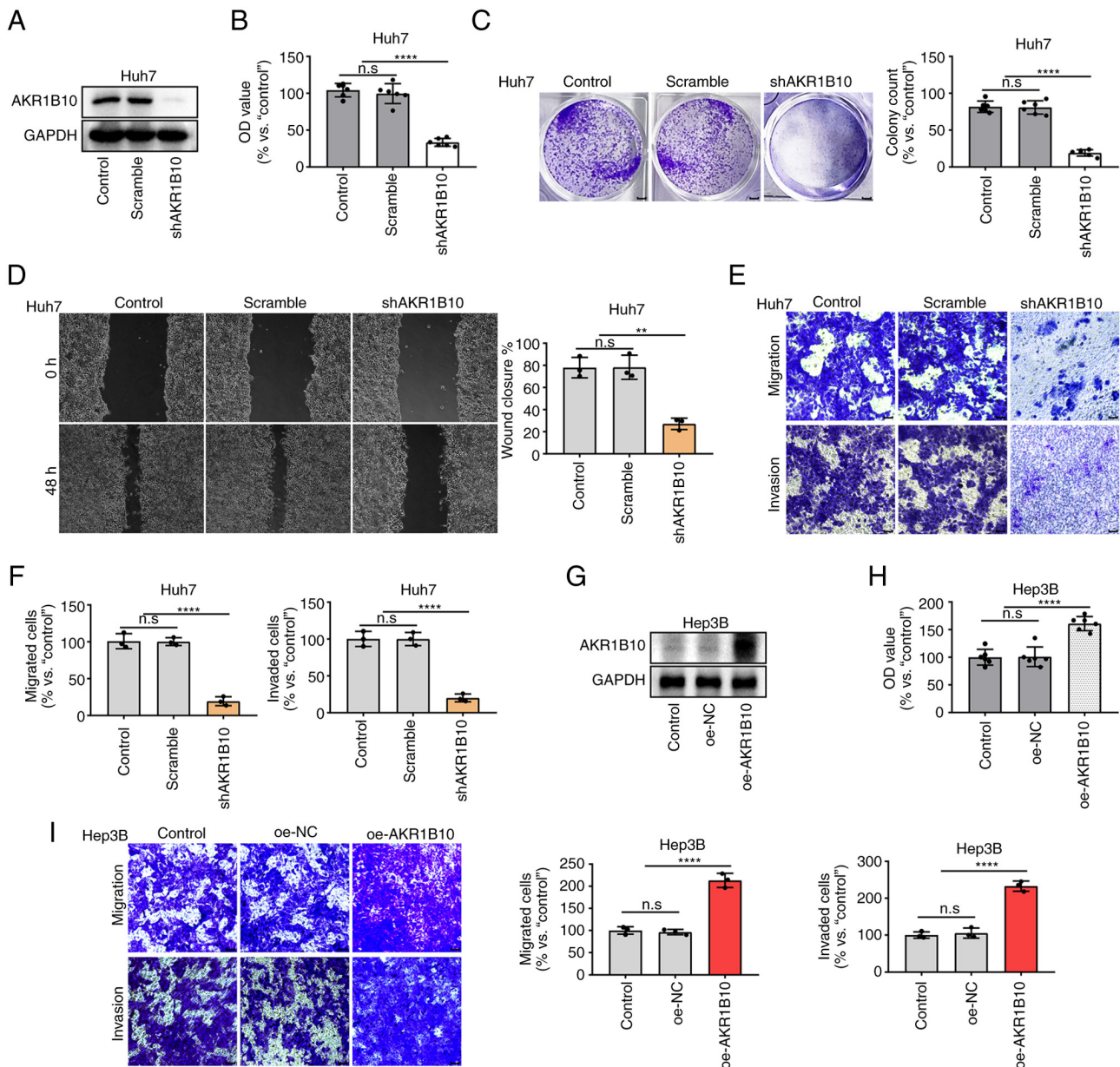
Figure 3. AKR1B10 promoted the proliferation, migration, and invasion in HCC cells. (A) AKR1B10 expression was knocked down in Huh7 cells and confirmed by western blotting. (B-F) AKR1B10 knockdown inhibits the proliferation, migration, and invasion of Huh7 cells. (G) AKR1B10 expression was overexpressed in Hep3B cells and confirmed by western blotting. (H-I) AKR1B10 overexpression promoted the proliferation, migration, and invasion of Hep3B cells. Cell proliferation was evaluated using a CCK-8 assay (B and H) and colony formation assays (C). Cell migration and invasion were investigated using Transwell assays (D, E, and I). **P<0.01 and ****P<0.0001. AKR1B10, aldo-keto reductase family 1 member B10; sh, short hairpin; oe, overexpression; NC, negative control; OD, optical density.

GDC-TCGA and DepMap analysis of co-expressed genes of AKR1B10, CCND1, and EMT-related genes. Since AKR1B10 was upregulated in HCC tissues and exhibited a notable influence on HCC cell behavior; therefore, its potential mechanisms in promoting this disease were assessed. Next, the association between AKR1B10 expression and the cell proliferation-related gene CCND1 (18,19) and EMT-related hub genes in GDC-TCGA tumor samples. The EMT-related hub genes were selected as E-cadherin, N-cadherin, Vimentin, and TWIST1. The results showed that all of the above genes were significantly associated with the expression of AKR1B10 (P<0.0001; Fig. 4A-E). Next, another dataset, DepMap, was selected for a similar correlation analysis. The expression of

E-cadherin (P=0.0217), N-cadherin (P=0.0245), and Vimentin (P=0.0073) genes in DepMap showed varying degrees of significant correlations with AKR1B10, apart from TWIST1 (P=0.7343; P-value cut-off=0.05; Fig. 4F-J).

AKR1B10 promotes the expression of CCND1 and EMT-related genes and activates the PI3K/AKT pathway. To further validate the above functions of AKR1B10, we measured the effects of AKR1B10 on the gene expression of CCND1 and EMT-related genes in HCC cells. AKR1B10 knockdown suppressed CCND1 expression and abrogated the cell cycle distribution in HCC cells (Fig. 5A and B). In addition, the expression of E-cadherin was increased, and
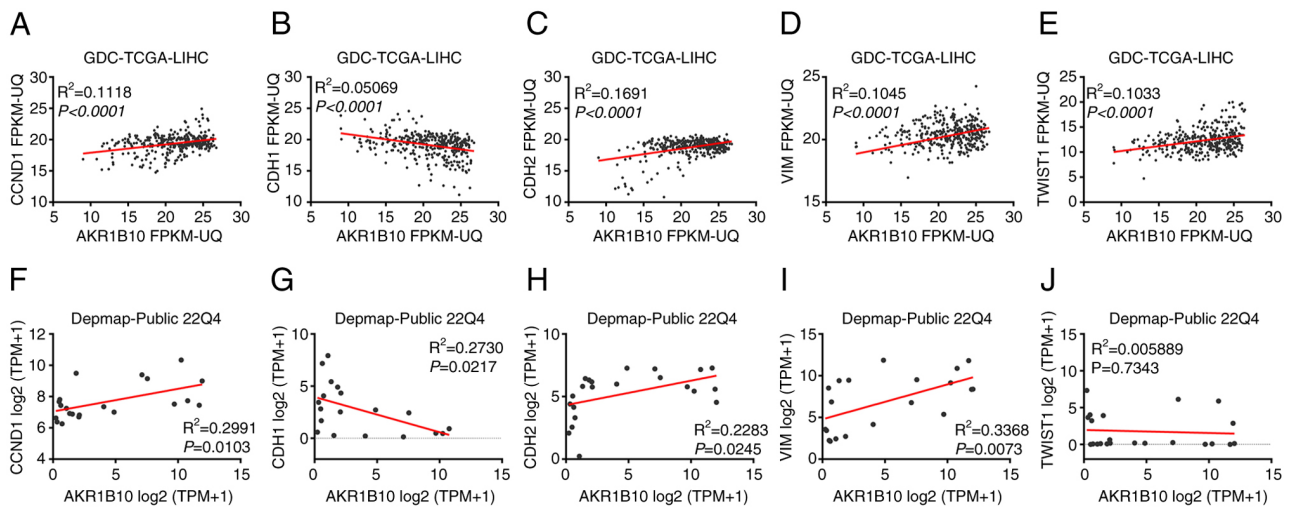
Figure 4. GDC-TCGA and DepMap analysis of the AKR1B10, CCND1, and EMT-related co-expressed genes. (A) Pearson correlation of AKR1B10 and CCND1 gene expression in the GDC-TCGA models. (B-E) Pearson correlation analysis of AKR1B10 and EMT-related gene expression in the GDC-TCGA models. (F) Pearson correlation analysis of AKR1B10 and CCND1 gene expression in the DepMap Public 22Q4 models. (G-J) Pearson correlation analysis of AKR1B10 and EMT-related gene expression in the DepMap Public 22Q4 models. AKR1B10, aldo-keto reductase family 1 member B10; EMT, epithelial-mesenchymal transition; GDC-TCGA, Genomic Data Commons-The Cancer Genome Atlas.
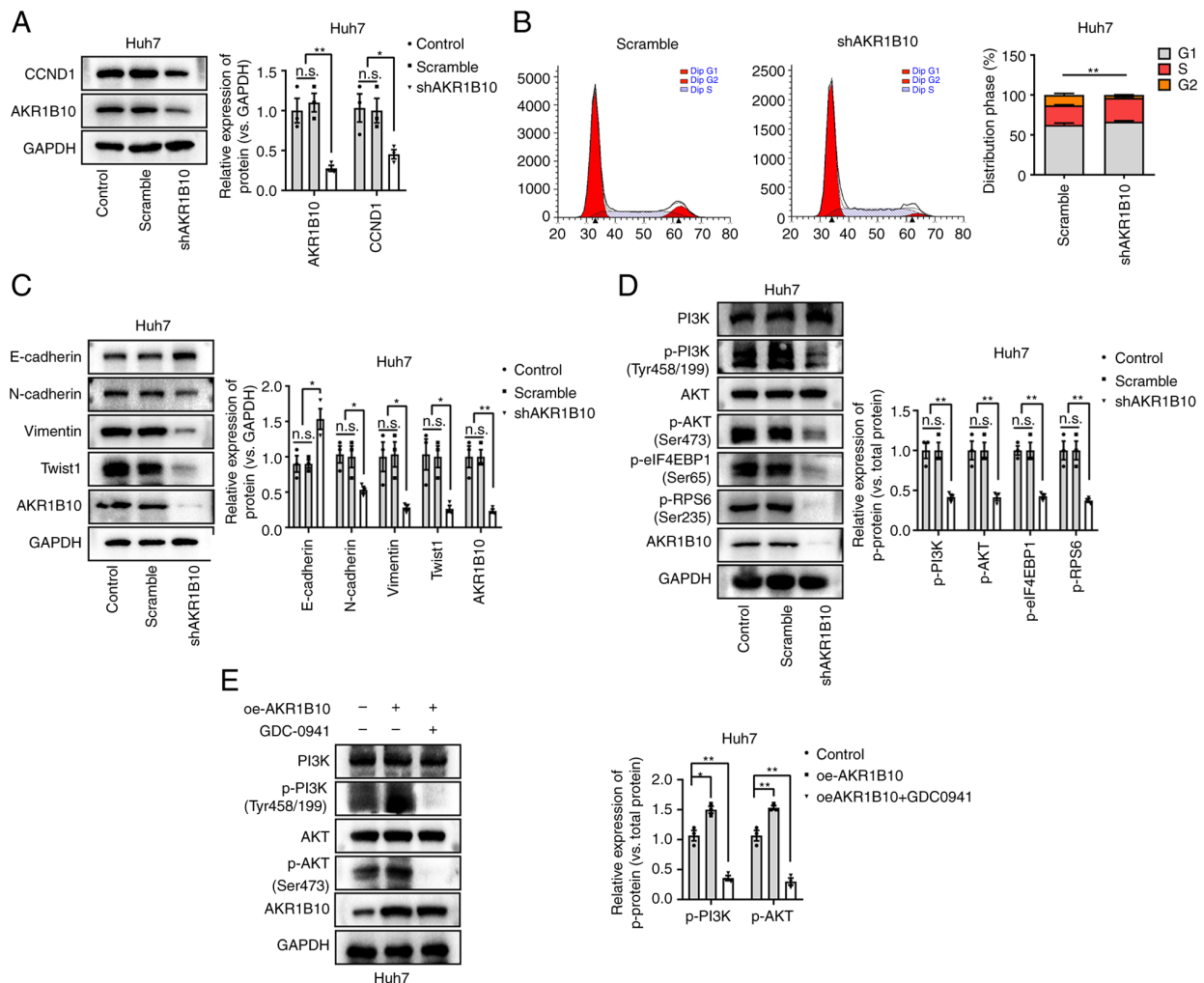

Figure 5. AKR1B10 promoted the expression of CCND1 and EMT-related genes and activate the PI3K/AKT pathway. (A) AKR1B10 knockdown inhibited the expression of CCND1 in Huh7 cells. (B) AKR1B10 knockdown disturbs cell cycle distribution in Huh7 cells. (C) AKR1B10 knockdown impairs the EMT of Huh7 cells. (D and E) Western blotting showed that the PI3K signal pathway was regulated by AKR1B10. AKR1B10-overexpressing Huh7 cells were incubated with 40 nM PI3K inhibitor GDC-0941 for 48 h, after which the expression of the PI3K signal pathway genes was measured using western blotting. $^*P<0.05$ and $^{**}P<0.01$. AKR1B10, aldo-keto reductase family 1 member B10; EMT, epithelial-mesenchymal transition; GDC-TCGA, Genomic Data Commons-The Cancer Genome Atlas; LIHC, liver hepatocellular carcinoma; TPM, transcripts per million; FPKM-UQ, the upper quartile Fragments Per Kilobase Million.

other EMT biomarkers, including N-cadherin, Vimentin, and TWIST-1, were downregulated after AKR1B10 knockdown (Fig. 5C). Based on these results, it is possible that AKR1B10 plays a significant role in the proliferation and EMT of HCC, affecting its proliferation, migration, and invasion.

As reported recently, AKR1B10 promotes tumor cell proliferation and migration through PI3K/AKT signaling (11). Furthermore, the degree of phosphorylation of proteins involved in the PI3K/AKT pathway was assessed, and it was found that phosphorylation was significantly reduced by AKR1B10 knockdown (Fig. 5D). Meanwhile, although cells transfected with AKR1B10 were subsequently treated with GDC-0941 (100 nM; PI3K/AKT pathway antagonist; MedChemExpress) for 24 h, western blotting showed that the protein content of AKR1B10 failed to be significantly altered (Fig. 5E). Based on these experiments, it was suggested that the PI3K/AKT signaling was involved in the pathological progression of HCC.

Discussion

HCC is one of the most common cancers in the world and the third leading cause of cancer-associated death (20). Due to delayed diagnosis and frequent cancer metastasis, the majority of HCC patients are diagnosed with advanced-stage cancer at the initial diagnosis (21). With the recent developments in biological therapies, the clinical treatment of HCC has seen progress; however, the survival benefits of these drug treatments for HCC patients still have several limitations. In particular, with immune checkpoint inhibitors as monotherapy for HCC patients, the outcomes to date have been disappointing (22). Furthermore, HCC is a heterogeneous disease with limited chemoradiotherapy treatment (7). The 5-year survival rate for patients with early-stage HCC has been reported to exceed 50% (2). Despite this, HCC has a poor 5-year overall survival rate (6). The limited value of existing biomarkers for diagnosing and treating HCC requires urgent identification of better biomarkers. Therefore, there is a crucial need to understand the molecular mechanisms underlying HCC development to identify better biomarkers and develop novel therapeutics.

As a member of the AKR1B family (9), the role of AKR1B10 in lung cancer (23,24), Renal Cell Carcinoma (25), ovarian cancer (26) and bladder cancer (27) carcinogenesis has been studied extensively. AKR1B10 is a cytosolic NADPH-dependent reductase, catabolizing various endogenous compounds by catalyzing the corresponding redox reactions (2). Research has shown that AKR1B10 contributes to cancer progression (11). Recent studies found that the overexpression of the enzyme in several types of cancer, including adrenocortical (10), breast (11), colon (12), and HCC (13,14). Subsequently, this study investigated its role in HCC. Through a comprehensive analysis of data from GDC-TCGA-PANCAN, GDC-TCGA-LIHC, and ICGC-LIRI databases, it was found that AKR1B10 expression was significantly upregulated pan-cancer and in HCC, and high expression was associated with shorter survival times (Fig. 2D-J), and confirmed that AKR1B10 was a potential biomarker for prognostic prediction of HCC. Studies have shown that cancer cells proliferate and migrate when AKR1B10 is knocked down (28,29). Additionally,

studies have shown that AKR1B10 expression is elevated in breast cancer and adrenocortical carcinoma tissues, where it is involved in proliferation, migration, and invasion (10,11). It should be noted that AKR1B10 may exhibit differing functions in different types of cells. Using the DepMap dataset, the gene effect CRISPR analysis, and the expression analysis of AKR1B10 in HCC cell lines, it was found that Huh7 cells were a potential excellent candidate for HCC cells. It was found in the present study that by knocking down AKR1B10 expression, Huh7 cells were less likely to proliferate, migrate, invade, and undergo EMT.

Different cellular processes rely on PI3K/AKT signaling, including cell proliferation, apoptosis, and migration (30,31). The PI3K/AKT pathway is reported to be regulated in the sustained activation of EMT in several types of cancer (32,33). PI3K/AKT-mediated EMT has been shown to promote HCC progression (34). Recently, there have been reports that AKR1B10 affects the activity of the PI3K pathway by regulating the substrate synthesis of PI3K in cancer cells (35,36). Previous studies demonstrated that AKR1B10-overexpressing breast cancer cells activated PI3K/AKT (11), thus, the association between AKR1B10 and PI3K/AKT signaling was assessed. Studies have reported various ways by which AKR1B10 promotes HCC proliferation, migration, and invasion (21,37). Additionally, AKRB10 may play a significant role in metabolic adaptation (2). While AKRB10 has been studied in HCC, the results were inconsistent. For example, AKR1B10 may play different roles depending on the HCC stage (9). Together, AKR1B10 may influence the progression of HCC through multiple signaling pathways associated with cell proliferation and migration. Finally, in the present study, it was found that AKR1B10 promoted HCC progression *in vitro* by upregulating the activity of the PI3K/AKT signaling pathway. Nevertheless, future studies are required using *in vivo* tumor models to verify the validity of the findings of the clinical tissue samples.

In conclusion, the results of the present study showed that AKR1B10 activated the PI3K/AKT pathway in Huh7 cells, and this resulted in increased proliferation, invasion, migration, and EMT.

Availability of data and materials

All data generated or analyzed during this study are included in this published article.

Authors' contributions

KT, ZL and HZ performed the experiments. YD collected the samples. ZL and HZ analyzed the data. HY conceived the study experiments and wrote the manuscript. KT and HY confirm the authenticity of all the raw data. All authors have read and approved the final manuscript.

Ethics approval and consent to participate

Not applicable.

Patient consent for publication

Not applicable.

Competing interests

The authors declare that they have no competing interests.

References

1. Ladd AD, Duarte S, Sahin I and Zarrinpar A: Mechanisms of drug resistance in HCC. Hepatology: Jan 3, 2023 (Epub ahead of print).
2. Wang Z, Pei Y, Li W, Zhang J and Liu J: Clinical value of AKR1B10 in hepatocellular carcinoma: A systematic review and meta-analysis. PLoS One 17: e0279591, 2022.
3. Siegel RL, Miller KD, Wagle NS and Jemal A: Cancer statistics, 2023. CA Cancer J Clin 73: 17-48, 2023.
4. Yu M, Chen Z, Zhou Q, Zhang B, Huang J, Jin L, Zhou B, Liu S, Yan J, Li X, *et al*: PARG inhibition limits HCC progression and potentiates the efficacy of immune checkpoint therapy. J Hepatol 77: 140-151, 2022.
5. Erstad DJ and Tanabe KK: Hepatocellular carcinoma: Early-stage management challenges. J Hepatocell Carcinoma 4: 81-92, 2017.
6. Yang MY, Hung TW, Wang CJ and Tseng TH: Inhibitory Effect of Nelumbo nucifera Leaf extract on 2-acetylaminofluorene-induced hepatocarcinogenesis through enhancing antioxidative potential and alleviating inflammation in rats. Antioxidants (Basel) 8: 329, 2019.
7. Huang H, Tsui YM and Ng IO: Fueling HCC dynamics: Interplay between tumor microenvironment and tumor initiating cells. Cell Mol Gastroenterol Hepatol 15: 1105-1116, 2023.
8. Cicinnati VR, Sotiropoulos GC and Beckebaum S: Established and emerging therapies for hepatocellular carcinoma. Minerva Med 101: 405-418, 2010.
9. DiStefano JK and Davis B: Diagnostic and prognostic potential of AKR1B10 in human hepatocellular carcinoma. Cancers (Basel) 11: 486, 2019.
10. Chen D, Huang R, Ren F, Wang H, Wang C and Zhang Y: FNDC5 and AKR1B10 inhibit the proliferation and metastasis of adrenocortical carcinoma cells by regulating AMPK/mTOR pathway. Exp Ther Med 25: 136, 2023.
11. Qu J, Li J, Zhang Y, He R, Liu X, Gong K, Duan L, Luo W, Hu Z, Wang G, *et al*: AKR1B10 promotes breast cancer cell proliferation and migration via the PI3K/AKT/NF-κB signaling pathway. Cell Biosci 11: 163, 2021.
12. Liu C, Shi L, Li W, Huang Z, Wang S, Xu P, Li T, Li Z, Luo F, Li W, *et al*: AKR1B10 accelerates the production of proinflammatory cytokines via the NF-κB signaling pathway in colon cancer. J Mol Histol 53: 781-791, 2022.
13. Ye X, Li C, Zu X, Lin M, Liu J, Xu G, Chen Z, Xu Y, Liu L, *et al*: A large-scale multicenter study validates aldo-keto reductase family 1 member B10 as a prevalent serum marker for detection of hepatocellular carcinoma. Hepatology 69: 2489-2501, 2019.
14. Xie C, Ye X, Zeng L, Zeng X and Cao D: Serum AKR1B10 as an indicator of unfavorable survival of hepatocellular carcinoma. J Gastroenterol 58: 1030-1042, 2023.
15. Xu B, Wang F, Song C, Sun Z, Cheng K, Tan Y, Wang H and Zou H: Large-scale proteome quantification of hepatocellular carcinoma tissues by a three-dimensional liquid chromatography strategy integrated with sample preparation. J Proteome Res 13: 3645-3654, 2014.
16. Kim SY, Shen Q, Son K, Kim HS, Yang HD, Na MJ, Shin E, Yu S, Kang K, You JS, *et al*: SMARCA4 oncogenic potential via IRAK1 enhancer to activate Gankyrin and AKR1B10 in liver cancer. Oncogene 40: 4652-4662, 2021.
17. Zhang J, Zhang X, Li J and Song Z: Systematic analysis of the ABC transporter family in hepatocellular carcinoma reveals the importance of ABCB6 in regulating ferroptosis. Life Sci 257: 118131, 2020.
18. Yang Z, Xu T, Xie T, Yang L, Wang G, Gao Y, Xi G and Zhang X: CDC42EP3 promotes glioma progression via regulation of CCND1. Cell Death Dis 13: 290, 2022.
19. Leontieva OV, Demidenko ZN and Blagosklonny MV: MEK drives cyclin D1 hyperelevation during geroconversion. Cell Death Differ 20: 1241-1249, 2013.
20. Siegel RL, Miller KD, Fuchs HE and Jemal A: Cancer statistics, 2021. CA Cancer J Clin 71: 7-33, 2021.
21. Zhang T, Guan G, Zhang J, Zheng H, Li D, Wang W, Lu F and Chen X: E2F1-mediated AUF1 upregulation promotes HCC development and enhances drug resistance via stabilization of AKR1B10. Cancer Sci 113: 1154-1167, 2022.
22. Romero D: Combination set to transform HCC therapy. Nat Rev Clin Oncol 17: 389, 2020.
23. Kim B, Lee HJ, Choi HY, Shin Y, Nam S, Seo G, Son DS, Jo J, Kim J, Lee J, *et al*: Clinical validity of the lung cancer biomarkers identified by bioinformatics analysis of public expression data. Oncotarget 67: 7431-7438, 2007.
24. Zhu D, Nie Y, Zhao Y, Chen X, Yang Z and Yang Y: RNF152 suppresses fatty acid oxidation and metastasis of lung adenocarcinoma by inhibiting IRAK1-Mediated AKR1B10 expression. Am J Pathol 193: 1603-1617, 2023.
25. Zheng L, Zhang X, Pan X, Huang Z, Zhang M, Xian J, Wei Y, Nie L, Zhang M, Gong J, *et al*: AKR1B10 is a new sensitive and specific marker for fumarate hydratase-deficient renal cell carcinoma. Mod Pathol 36: 100303, 2023.
26. Hojnik M, Šuster NK, Smrkolj Š, Sisinger D, Grazio SF, Verdenik I and Rižner TL: AKR1B1 as a prognostic biomarker of high-grade serous ovarian cancer. Cancers (Basel) 14: 809, 2022.
27. Huang Z, Yan Y, Zhu Z, Liu J, He X, Dalangood S, Li M, Tan M, Cai J, Tang P, *et al*: CBX7 suppresses urinary bladder cancer progression via modulating AKR1B10-ERK signaling. Cell Death Dis 12: 537, 2021.
28. Shao X, Wu J, Yu S, Zhou Y and Zhou C: AKR1B10 inhibits the proliferation and migration of gastric cancer via regulating epithelial-mesenchymal transition. Aging (Albany NY) 13: 22298-22314, 2021.
29. Yao Y, Wang X, Zhou D, Li H, Qian H, Zhang J, Jiang L, Wang B, Lin Q and Zhu X: Loss of AKR1B10 promotes colorectal cancer cells proliferation and migration via regulating FGF1-dependent pathway. Aging (Albany NY) 12: 13059-13075, 2020.
30. He Y, Sun MM, Zhang GG, Yang J, Chen KS, Xu WW and Li B: Targeting PI3K/Akt signal transduction for cancer therapy. Signal Transduct Target Ther 6: 425, 2021.
31. Yang J, Nie J, Ma X, Wei Y, Peng Y and Wei X: Targeting PI3K in cancer: Mechanisms and advances in clinical trials. Mol Cancer 18: 26, 2019.
32. Wang C, Yang Z, Xu E, Shen X, Wang X, Li Z, Yu H, Chen K, Hu Q, Xia X, *et al*: Apolipoprotein C-II induces EMT to promote gastric cancer peritoneal metastasis via PI3K/AKT/mTOR pathway. Clin Transl Med 11: e522, 2021.
33. Wang Y, Li Y, Wang L, Chen B, Zhu M, Ma C, Mu C, Tao A, Li S, Kang L, *et al*: Cinnamaldehyde suppressed EGF-Induced EMT process and inhibits ovarian cancer progression through PI3K/AKT pathway. Front Pharmacol 13: 779608, 2022.
34. Dian MJ, Li J, Zhang XL, Li ZJ, Zhou Y, Zhou W, Zhong QL, Pang WQ, Lin XL, Liu T, *et al*: MST4 negatively regulates the EMT, invasion and metastasis of HCC cells by inactivating PI3K/AKT/Snail1 axis. J Cancer 12: 4463-4477, 2021.
35. Huang C, Cao Z, Ma J, Shen Y, Bu Y, Khoshaba R, Shi G, Huang D, Liao DF, Ji H, *et al*: AKR1B10 activates diacylglycerol (DAG) second messenger in breast cancer cells. Mol Carcinog 57: 1300-1310, 2018.
36. Manning BD and Toker A: AKT/PKB signaling: Navigating the network. Cell 169: 381-405, 2017.
37. Wu T, Ke Y, Tang H, Liao C, Li J and Wang L: Fidarestat induces glycolysis of NK cells through decreasing AKR1B10 expression to inhibit hepatocellular carcinoma. Mol Ther Oncolytics 23: 420-431, 2021.